MORPHOLOGICAL SYNTHESIS OF ECG SIGNALS FOR PERSON AUTHENTICATION

Gary Garcia Molina, Fons Bruekers, Cristian Presura, Marijn Damstra, and Michiel van der Veen

Information and System Security, Philips Research Europe
High Tech Campus 34, 5656AE, Eindhoven, Netherlands
email: {gary.garcia, fons.bruekers, cristian.presura, marijn.damstra, and michiel.van.der.veen}@philips.com

ABSTRACT

In this paper, we propose a novel approach using the morphological properties of the R-R segments in an ECG signal for biometric authentication. The authenticity of a given R-R segment is decided by comparing it to a matching R-R segment morphologically synthesized from a model characterizing the identity to be authenticated. The morphological synthesis process uses a set of R-R segments (templates), recorded during enrolment at different heart-rates, and a time alignment algorithm. This ensures the authentication to be independent of the, usually variable, heart-rate. The optimum average equal-error-rate obtained in our experiments is 2%.

1. INTRODUCTION

Person authentication has traditionally been achieved by means of passwords, tokens or PINs, i.e. something that the person possesses. Biometrics permits to authenticate a person using his/her inherent individual characteristics, i.e. something that the person is or produces. Common biometric modalities include fingerprints, voice, facial geometry, or iris. Also electrocardiogram signals (ECG), which reflect the electrical activity of the heart, appear to have a promising potential for biometric applications as shown by the identification results reported in [1, 2, 3, 4].

ECG signals are mainly used in diagnosis but they vary from person to person according to different factors such as anatomic differences in the heart, gender, relative body weight, and chest configuration [4]. Detailed clinical diagnosis requires the ECG to be recorded using ten electrodes out of which twelve electrical potential differences (leads) are derived. In the framework of biometric applications a single lead appears to be sufficient [1, 4]. At present, portable ECG monitors that do not require using conductive gel (dry-electrode devices) are commercially available. This opens the possibility for devising convenient biometric appliances based on mere skin contact.

A biometric authentication system is implemented by comparing a measurement of a biometric to its *model* which results from an *enrollment phase*. The comparison, in ECG-based biometrics, relies on the characteristics of the PQRST-cycles (see Fig. 2a) that compose an ECG recording. Current approaches are based on the extraction of features from a PQRST-cycle [1, 2, 3, 4], in particular the relative location and amplitudes of the P, Q, R, S, and T peaks (Fig. 2a). In practice such peaks cannot be precisely determined in an automated way, e.g. when they do not clearly appear in the signal as a result of certain electrode configurations, in pathological cases or when the noise level is high. Furthermore the finite sampling frequency and errors in the detection procedures contribute to the uncertainty in the determination of the peak locations.

Rather than determining the peaks locations for feature extraction, we use the morphology of R-R segments (i.e. the shape of the signal that is defined by the relative positions of the characteristic points of the PQRST-cycle) as a means for comparison between a biometric measurement and a model. The R-peaks are taken as reference because they are present in every electrode configuration and can be more precisely and unambiguously determined as they constitute the highest peaks in the ECG signal. Furthermore, all the elements of a PQRST-cycle are contained within an R-R segment. Whereas the relative location of the distinctive patterns in a PQRST-cycle can change as a result of the heart-rate variability, the morphology of R-R segments remains essentially unchanged.

In this paper we investigate the use of R-R segments morphology to achieve biometric authentication by obtaining an equal-error-rate (EER). This approach is tested in our own database consisting of ten subjects. While larger ECG databases are available online, they are primarily intended for clinical applications since they mainly contain ECGs affected by heart conditions. Thus, performing biometric classification on such databases could rather lead to the recognition of diseases.

The rest of this paper is organized as follows. Section 2 presents the basic structure of the biometric authentication system based on the morphological comparison of R-R segments and introduces the notion of morphological synthesis. In Section 3 the preprocessing and R-R segmentation are discussed. Section 4 describes the algorithm for morphological R-R segments synthesis. We present our experimental results and conclusion in Sections 5 and 6 respectively.

2. MORPHOLOGICAL ECG-BASED AUTHENTICATION

Biometric authenticity is decided on the basis of a score that quantifies the resemblance between a biometric measurement and the model associated with the enrolled subject (denoted by i) whose identity was claimed. Such score is obtained as depicted in Fig. 1.

The digitized ECG signal is first preprocessed and segmented into R-R segments (see Section 3). For each R-R segment (s), the corresponding R-R length (ρ) is determined (for convenience we quantify the duration of a digital signal in terms of its length in number of samples).

The current R-R segment is amplitude and length normalized so that its sample-values are scaled in the range $[-1;+1]$ and it contains L (*length-normalization parameter*) samples.

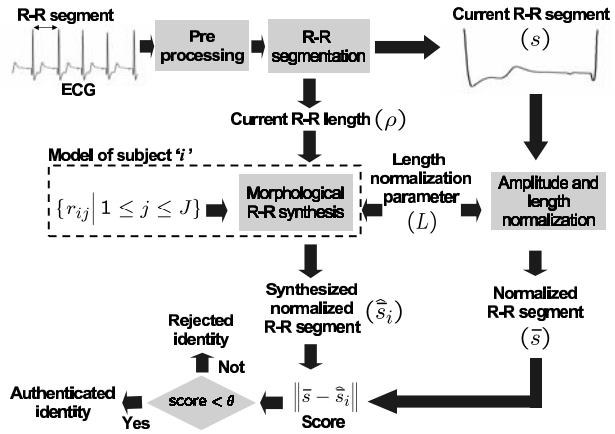

Fig. 1. Morphological ECG-based authentication

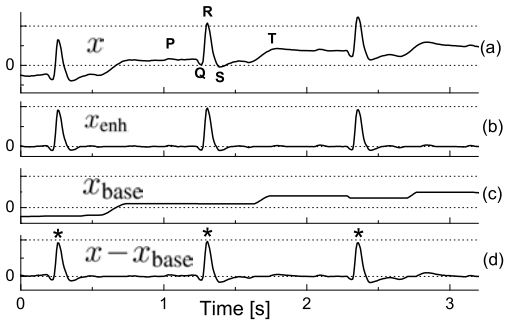

Fig. 2. R-R segmentation

The amplitude normalization is done by dividing the positive (resp. negative) samples by the absolute value of the maximum (resp. minimum) sample-value in the current R-R segment. Because of the heart-rate variability, the R-R segments have in general different lengths. We normalize the length of each R-R segment using standard spline-fitting interpolation so as to get L equidistant points. Henceforth the normalized version of any signal is denoted using the "$\bar{}$" symbol. Thus, $\bar{s}$ is the normalized version of s.

An estimate of the normalized version of s denoted as $\hat{\bar{s}}_i$ is morphologically synthesized using the length-normalization parameter L, the current R-R length ρ, and the elements in the set $\{r_{i,j} \mid 1 \le j \le J\}$ where the number of elements $J \ge 2$ is the *model order*. The model of subject i consists of the set of enrolled *templates* $\{r_{i,j}\}$ (having respective lengths $\{\rho_{i,j}\}$) and the morphologic synthesis algorithm. A particular choice for the morphologic synthesis algorithm is described in Section 4. Another approach to morphologically synthesize ECG signals can be found in [5].

The similarity score between s and the model is equal to the l_2-norm of $\bar{s}$ and $\hat{\bar{s}}_i$, i.e. $\|\bar{s} - \hat{\bar{s}}_i\|$. To decide the authenticity of the claimed identity this score is usually compared to a threshold θ. The identity is authenticated if $\|\bar{s} - \hat{\bar{s}}_i\| < \theta$. The threshold is set depending on the application and trades security versus convenience (see Section 5).

3. PREPROCESSING AND R-R SEGMENTATION

Prior to detecting the R peaks, the ECG signal is preprocessed using a Savitzky-Golay (SG) time-domain smoothing filter [6]. This is a standard filter choice in ECG signal processing which fits a polynomial function to the data surrounding each sample and replaces it by the value of its fitted polynomial.

Among the various approaches [7] used to automatically identify the constitutive elements of a PQRST-cycle, we focus on the algorithm described in [8]. This algorithm preserves the sharp components in the signal, can effectively remove baseline drifts, does not require any specific assumptions other than the sharpness of the peaks and valleys constituting the PQRST-cycle, and is computationally efficient.

In Fig. 2 we briefly sketch the processing steps leading to the R-R segmentation. An in-depth description of this process can be found in [8]. In Fig. 2a a preprocessed ECG signal (x) is shown. A significant baseline drift is apparent in such signal. To detect the R peaks, an R-peak enhanced signal (x_{enh}) is derived from x (Fig. 2b). This signal allows for straightforward R-peak detection using simple thresholding. The baseline drift is removed using a baseline estimate signal denoted as x_{base} (Fig. 2c) which is subtracted from x to derive the baseline-corrected signal in Fig. 2d. The R-R segments are delimited by the '*' symbols in Fig. 2d.

4. MORPHOLOGICAL R-R SYNTHESIS

We formalize the process of morphologically synthesizing R-R segments as follows. Given a set of R-R templates sharing a common morphology: $\{r_{i,j} \mid 1 \le j \le J\}$ (e.g. the set associated with the model of subject i) with respective lengths $\{\rho_{i,j} \mid \rho_{i,j} < \rho_{i,j+1}\}$ and the current R-R length ρ, we seek to generate a normalized R-R segment $\hat{\bar{s}}_i$ that has the same morphology as the elements in $\{\bar{r}_{i,j}\}$. The case $\rho \in \{\rho_{i,j}\}$ is trivial as $\hat{\bar{s}}_i$ is equal to $\bar{r}_{i,j}$ such that $\rho_{i,j} = \rho$.

When $\rho \notin \{\rho_{i,j}\}$ the morphological synthesis problem is solved using the notion of time alignment for comparing two signals. Time alignment is essentially used to match morphologically close signals that do not evolve at the same pace. Time alignment algorithms include *linear time normalization* and *dynamic time warping* [9] (DTW). The latter is used here.

DTW is mainly used in speech applications to achieve time alignment between a reference signal and a test signal whose time scales are not aligned. Thus, DTW results in a nonlinear warping *path* that compensates for local compression or expansion of the time scale. In Fig. 3, we depict the path corresponding to the normalized versions of two "morphologically close" R-R segments denoted as $\bar{x}_1$ and $\bar{x}_2$. The reference signal $\bar{x}_1$ and the test signal $\bar{x}_2$ are reported in the vertical and horizontal axes respectively. The path (denoted as $P_{\bar{x}_1,\bar{x}_2}$) exhibits diagonal segments in the regions corresponding to similar patterns in $\bar{x}_1$ and $\bar{x}_2$, and horizontal or vertical segments where the signals do not align.

For our purposes we slightly modified the DTW algorithm by removing vertical segments in order to make $P_{\bar{x}_1,\bar{x}_2}$ a function from the $\bar{x}_2$-domain into the $\bar{x}_1$-domain. Thus, a vertical segment was replaced by a single point corresponding to the mean vertical value along the considered segment.

Using the fact that $P_{\bar{x}_1,\bar{x}_2}$ aligns matching temporal patterns, an estimate for the test signal $\bar{x}_2$ (denoted as $\hat{\bar{x}}_2$) can be obtained from the reference signal $\bar{x}_1$ and the path $P_{\bar{x}_1,\bar{x}_2}$. If

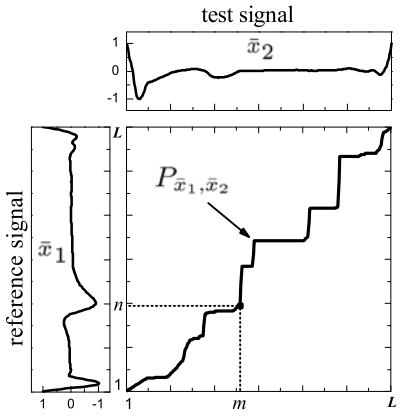

Fig. 3. Path $P_{\bar{x}_1,\bar{x}_2}$ between $\bar{x}_1$ and $\bar{x}_2$

$n = P_{\bar{x}_1,\bar{x}_2}(m)$ then the following relations hold:

$$\begin{array}{rcl} \hat{\bar{x}}_2(m) & = & \bar{x}_1(n) \\ \Rightarrow \quad \hat{\bar{x}}_2(m) & = & \bar{x}_1(P_{\bar{x}_1,\bar{x}_2}(m)) \; ; \; m = 1,\ldots,L. \end{array} \tag{1}$$

The relations in (1) serve as basis for synthesizing $\hat{\bar{s}}_i$ from $\{r_{i,j}\}$. By arbitrarily choosing a reference template (denoted as $r_{i,k}$) in $\{r_{i,j}\}$ and replacing x_1 (resp. x_2) by $r_{i,k}$ (resp. s_i) in (1), we have:

$$\hat{\bar{s}}_i(m) = \bar{r}_{i,k}(P_{\bar{r}_{i,k},\bar{s}_i}(m)) \quad ; \quad m = 1,\ldots,L. \tag{2}$$

To estimate the path $P_{\bar{r}_{i,k},\bar{s}_i}$, we consider the association between each template length $\rho_{i,j}$ with its respective (*inter-template*) path $P_{\bar{r}_{i,k},\bar{r}_{i,j}}$ with $r_{i,k}$ as reference. For each positive integer ρ, such path can be estimated from the inter-template paths, the template lengths and ρ. Thus, an estimate for $P_{\bar{r}_{i,k},\bar{s}_i}$ (denoted as $\hat{P}_{\bar{r}_{i,k},\bar{s}_i}$) can be obtained through a functional $\mathscr{F}$:

$$\hat{P}_{\bar{r}_{i,k},\bar{s}_i} = \mathscr{F}(P_{\bar{r}_{i,k},\bar{r}_{i,1}},\ldots,P_{\bar{r}_{i,k},\bar{r}_{i,J}},\rho_{i,1},\ldots,\rho_{i,J},\rho). \tag{3}$$

A particular choice for $\mathscr{F}$, which we adopt here, corresponds to a linear combination of the inter-template paths (4).

$$\hat{P}_{\bar{r}_{i,k},\bar{s}_i}(m) = \sum_{j=1}^{J} \alpha_{i,j} P_{\bar{r}_{i,k},\bar{r}_{i,j}}(m) \quad ; \quad \alpha_{i,j} \in \mathbb{R}, \tag{4}$$

where each coefficient $\alpha_{i,j}$ depends on the template lengths and ρ. For notation convenience we do not explicitly denote such dependency.

The monotonicity of $\hat{P}_{\bar{r}_{i,k},\bar{s}_i}$ can be ensured by constraining the weighting coefficients $\alpha_{i,j}$ or by post-processing. A possible form of post-processing can be defined as follows:

$$\begin{array}{rcl} \hat{P}'_{\bar{r}_{i,k},\bar{s}_i}(m) = & \left[\!\!\left[\displaystyle\sum_{j=1}^{J} \alpha_{i,j} P_{\bar{r}_{i,k},\bar{r}_{i,j}}(m) \right]\!\!\right] \\ \hat{P}_{\bar{r}_{i,k},\bar{s}_i}(m) = & \max(\hat{P}_{\bar{r}_{i,k},\bar{s}_i}(m-1), \hat{P}'_{\bar{r}_{i,k},\bar{s}_i}(m)), \end{array} \tag{5}$$

where $2 \leq m \leq L$, $\hat{P}_{\bar{r}_{i,k},\bar{s}_i}(1) = \hat{P}'_{\bar{r}_{i,k},\bar{s}_i}(1)$ and $[\![\cdot]\!]$ is the nearest integer function. Using the estimated $\hat{P}_{\bar{r}_{i,k},\bar{s}_i}$ in (2), yields:

$$\hat{\bar{s}}_i(m) = \bar{r}_{i,k}\left(\hat{P}_{\bar{r}_{i,k},\bar{s}_i}(m)\right). \tag{6}$$

A possible approach for obtaining the linear combination coefficients $\alpha_{i,j}$ consists in using the Lagrange interpolation formula:

$$\alpha_{i,j} = \prod_{l \neq j} \frac{\rho - \rho_{i,l}}{\rho_{i,j} - \rho_{i,l}}. \tag{7}$$

Instead of using the full set of templates to determine the $\alpha_{i,j}$'s (*full template selection* FTS), it is possible to select only two neighboring templates $r_{i,k}, r_{i,k+1}$ in $\{r_{i,j}\}$ depending on ρ (*neighboring template selection* (NTS)). The lengths of the chosen templates are such that: $\rho_{i,k} < \rho < \rho_{i,k+1}$. If $\rho < \rho_{i,1}$ ($\rho > \rho_{i,J}$) then $k = 1$ ($k = J-1$). $\hat{P}'_{\bar{r}_{i,k},\bar{s}_i}(m)$ can then be determined from (5) by setting $\alpha_{i,j}\big|_{j \neq k,k+1} = 0$:

$$\begin{array}{rcl} \hat{P}'_{\bar{r}_{i,k},\bar{s}_i}(m) & = & \left[\!\!\left[\alpha_{i,k} P_{\bar{r}_{i,k},\bar{r}_{i,k}}(m) + \alpha_{i,k+1} P_{\bar{r}_{i,k},\bar{r}_{i,k+1}}(m) \right]\!\!\right] \\ & = & \left[\!\!\left[\alpha_{i,k} m + \alpha_{i,k+1} P_{\bar{r}_{i,k},\bar{r}_{i,k+1}}(m) \right]\!\!\right], \end{array} \tag{8}$$

where $\alpha_{i,k} = \frac{\rho - \rho_{i,l}}{\rho_{i,k} - \rho_{i,l}}$ and $\alpha_{i,k+1} = 1 - \alpha_{i,k}$. Thus, $\alpha_{i,k}, \alpha_{i,k+1}$ relate to linear interpolation.

5. RESULTS

The ECG signals for our experiments were acquired at a sampling frequency of 128 Hz by means of two electrodes placed on both wrists using the dry-electrode ECG acquisition device described in [10]. An anti-aliasing filter and a power-line notch-filter are embedded in the device.

Ten subjects participated in five five-minute long experimental sessions distributed over four weeks. Subjects were instructed to remain sufficiently quiet so as to reduce muscular noise. Two-hundred noise-free R-R segments per subject were manually selected to obtain the EER corresponding to the authentication based on a single R-R segment.

The EER is a common biometric performance indicator which corresponds to the rate at which the false accept rate (FAR, i.e the fraction of R-R segments incorrectly authenticated) is equal to the false reject rate (FRR, i.e. the fraction of R-R segments incorrectly rejected). FAR and FRR can be traded using the threshold θ.

We estimated the EER for each subject as the average of a ten-fold cross-validation. The R-R segments of each subject were randomly divided into ten groups and ten estimates for the EER were obtained. In each estimate one group was set apart for building the biometric model and the remaining (nine) groups along with nine groups corresponding to each of the other nine subjects were used to compute the EER.

Given a cross-validation group, the J templates for the biometric model were chosen so that their lengths were (approximately) uniformly distributed between the lengths of the shortest and longest R-R segments in the group. The number of templates was chosen to be equal for each enrolled-subject's model.

Different combinations for the length-normalization and model order parameters were tested in terms of the average EER across subjects. In Fig. 4 we depict the average EERs resulting from using FTS (unfilled symbols) and NTS (filled symbols).

The EER associated with FTS has a tendency to increase with the model order for each choice of L. The lowest EER corresponds to $J = 2$ and $L = 300$. The linear interpolation appears then to be optimal. This result leads to the NTS approach in which only linear interpolations are performed.

For $J = 2$ both approaches give the same result. However, the EER for the NTS is noticeably lower for higher J regardless of L. The lowest EER is equal to 0.033 for $L = 300$ and $J = 2$. The optimum value for L is 300 for both approaches. From our results it appears that increasing J beyond 5, does not lead to an important decrease in EER. This suggest that building a biometric model necessitates only few R-R segments whose lengths must conveniently be chosen between the longest (corresponding to the lowest heart-rate) and shortest (corresponding to highest heart-rate) possible lengths. Thus, a possible enrolling strategy can consist in eliciting low and high heart-rates through relaxation and physical activity.

To investigate the increasing trend (with the model order) of the EER associated with the FTS approach, the EERs are computed when the required length is inside and outside the interval defined by the shortest and longest templates. These cases are respectively referred to as interpolation and extrapolation. In Table 1, we report the EERs associated to few combinations of L and J for interpolation and extrapolation corresponding to the FTS and NTS approaches. In every case, the extrapolation-EER is higher than the corresponding interpolation-EER. The lowest EER (2%) occurs for the interpolation in the NTS approach. This result remains constant for different model orders and length-normalization values.

Comparing the extrapolation-EERs for both FTS and NTS leads to the following observations. First, the extrapolation-EER is higher in FTS than in NTS for each pair L, J. Second, the extrapolation-EER increases faster with J in the FTS approach.

Extrapolation leads to higher EER for both FTS and NTS. Possible solutions to handle this issue are: discarding those R-R segments whose lengths lead to extrapolation or ensure that the enrolment procedure includes templates with extreme lengths.

Biometric modalities for authentication are evaluated according to different criteria among which we mention EER, convenience, privacy concerns, and identity theft deterrence. As far as EER is concerned, the early results of our approach can compare with hand-geometry (0.01), face (0.03), and fingerprint (0.05) based authentication [11]. Yet, ECG offers advantages in terms of convenience and identity theft deterrence. Indeed, the ECG can be simply acquired through holding two electrodes for few seconds. In addition, it appears to be difficult counterfeiting someone's ECG without the help of sophisticated equipment.

Privacy concerns apply to the proposed ECG-based authentication system, since it is required to store templates in the system. Such storage can be nevertheless made secure by using cryptographic techniques specially developed for biometric applications [12].

6. CONCLUSIONS AND FUTURE WORK

In this paper we used the morphological characteristics of R-R segments to achieve biometric authentication. The resemblance between an R-R segment and a biometric model was quantified by means of a novel algorithm that allowed us to morphologically synthesize a matching R-R segment in function of the current heart-rate. Thus, the authentication was made independent of the (usually variable) heart-rate.

The optimal approach and parameters choice for the morphological synthesis were defined in function of the biometric performance in terms of EERs. Thus, the dynamic selection of elements in the biometric model in function of the current heart-rate appears to bring the lowest EER.

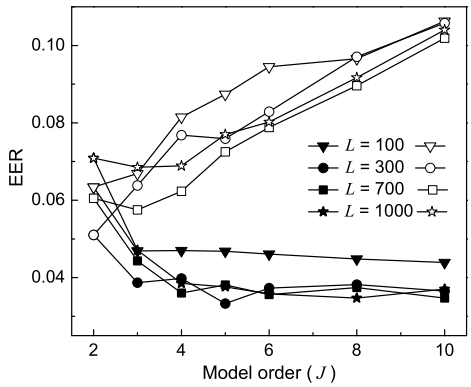

Fig. 4. Average EER across subjects, FTS (unfilled symbols), NTS (filled symbols)

	FTS		NTS	
	Interp.	Extrap.	Interp.	Extrap.
$L = 300, J = 6$	0.046	0.092	0.022	0.061
$L = 300, J = 8$	0.050	0.127	0.022	0.071
$L = 300, J = 10$	0.056	0.157	0.022	0.084
$L = 700, J = 6$	0.045	0.074	0.021	0.059
$L = 700, J = 8$	0.050	0.116	0.022	0.052
$L = 700, J = 10$	0.052	0.165	0.021	0.073

Table 1. EERs associated with extrapolation and interpolation for the FTS and NTS approaches

In order to deal with degraded EERs caused by extrapolation, those R-R segments with lengths outside the interval defined by the shortest and longest templates can be discarded. This can lead to a substantial improvement of the EER. In our experiments the EER decreased from 3% to 2% (see Fig. 4 and Table 1).

Another strategy to limit the extrapolation effect would consist in ensuring that the enrolment procedure includes R-R templates having extreme lengths. This can be achieved by eliciting low and high heart-rates through relaxation and physical activity.

Authentication was done on the basis of a single R-R segment. This can be extended to a sequence of R-R segments. Thereby further decreases in EER are expected.

To evaluate further the validity of our approach, the algorithms presented in this paper are being tested in a database comprising more subjects with measurements taken during a longer time span to take into account ECG differences across time.

REFERENCES

[1] Lena Biel, Ola Pettersson, Lennart Philipson, and Peter Wide, "ECG Analysis: A New Approach in Human Identification," *IEEE Transactions on Instrumentation and Measurement*, vol. 50, no. 3, pp. 808–812, 2001.

[2] S.A. Israel, W.T. Scruggs, W.J. Worek, and J.M. Irvine, "Fusing Face and ECG for Personal Identification,"

in *Proceedings of the 32nd Applied Imagery Pattern Recognition Workshop (AIPR 03)*, 2003.

[3] S.A. Israel, J.M. Irvine, A. Cheng, M.D. Wiederhold, and B.K. Wiederhold, "ECG to identify individuals," *Pattern Recognition*, vol. 38, no. 1, pp. 133–142, 2005.

[4] T.W. Shen, W.J. Tompkins, and Y.H. Hu, "One-Lead ECG for Identity Verification," *Proceedings of the Second Joint EMBS/BMES Conference*, pp. 62–63, 2002.

[5] A.J. Nimunkar and W.J. Tompkins, "ECG synthesis based on morphing," in *Proceedings of the 26th Annual International Conference of the Engineering in Medicine and Biology Society EMBC*, 2004, vol. 2, pp. 879–881.

[6] J. Luo, K. Ying, P. He, and J. Bai, "Properties of Savitzky Golay digital differentiators," *Digital Signal Processing*, vol. 2, no. 15, pp. 122–136, 2005.

[7] B.-U. Köhler, C. Henning, and R. Orglmeister, "The Principles of Software QRS Detection," *IEEE Engineering in medecine and Biology*, vol. 21, no. 1, pp. 42–57, 2002.

[8] P.E. Trahanias, "An Approach to QRS Complex Detection Using Mathematical Morphology," *IEEE Transactions on Biomedical Engineering*, vol. 40, no. 2, pp. 201–205, 1993.

[9] H. Sakoe and S. Chiba, "Dynamic programming algorithm optimization for spoken word recognition," *IEEE Trans. Acoustics, Speech, Signal Processing*, vol. 26, no. 1, pp. 43–49, 1978.

[10] F. van de Bovenkamp, "Heart tuner pro-04 user guide," http://www.heartcoherence.com/userguide/pro04UserGuide.htm.

[11] T. Mansfield, G. Kelly, D. Chandler, and J. Kane, "Biometric Product Testing Final Report," http://www.cesg.gov.uk/site/ast/biometrics/media/BiometricTestReportpt1.pdf, 2001.

[12] P. Tuyls, A. H. M. Akkermans, T. A. M. Kevenaar, G-J. Schrijen, A. M. Bazen, and R. N. J. Veldhuis, "Practical biometric authentication with template protection," in *5th Int. Conf. on Audio- and Video-Based Personal Authentication (AVBPA)*, July 2005, vol. LNCS 3546, pp. 436–446.